

Sevoflurane-Induced Structural Changes in a Four- α -Helix Bundle Protein[†]Ravindernath Pidikiti,[‡] Tao Zhang,[‡] Krishna M. G. Mallela,[§] Mohammad Shamim,^{||} Konda S. Reddy,[§] and Jonas S. Johansson^{*,†,§,⊥}*Departments of Anesthesiology and Critical Care Medicine, Biochemistry and Biophysics, and Internal Medicine and Johnson Research Foundation, University of Pennsylvania, Philadelphia, Pennsylvania 19104**Received May 13, 2005; Revised Manuscript Received July 5, 2005*

ABSTRACT: The mechanisms whereby volatile general anesthetics reversibly alter protein function in the central nervous system remain obscure. Using three different spectroscopic approaches, evidence is presented that binding of the modern general anesthetic sevoflurane to the hydrophobic core of a model four- α -helix bundle protein results in structural changes. Aromatic residues in the hydrophobic core reorient into new environments upon anesthetic binding, and the protein as a whole becomes less dynamic and exhibits structural tightening. Comparable structural changes in the predicted in vivo protein targets, such as the γ -aminobutyric acid type A receptor and the *N*-methyl-D-aspartate receptor, may underlie some, or all, of the behavioral effects of these widely used clinical agents.

In the United States alone, on the order of 20 million general anesthetics are administered annually (1). Nevertheless, molecular mechanisms of volatile general anesthetic action remain remarkably obscure despite widespread and longstanding clinical use. The currently favored targets for these drugs include the Cys-loop ligand-gated ion channels such as the γ -aminobutyric acid type A receptor and the homologous glycine receptor (2–4). Although the structures of these membrane proteins remain unclear, recent electron cryomicroscopy studies on the related nicotinic acetylcholine receptor from *Torpedo marmorata* at 4 Å resolution indicate that the transmembrane domains of each subunit consist of a four- α -helix bundle (5, 6). The expressed four- α -helix bundle ($\text{A}\alpha_2$ -L1M/L38M)₂¹ (Figure 1A) is therefore proposed to serve as a scaled-down model for the transmembrane domains of these and other membrane proteins. The rationale for this approach is supported by the evidence that the plasma membrane-embedded regions of proteins such as the nicotinic acetylcholine receptor (7, 8), the γ -aminobutyric acid type A receptor (9), and bovine rhodopsin (10) may interact directly with volatile general anesthetics. One of the key advantages of studying such a structural motif in isolation is that it is possible to use a variety of spectroscopic techniques that cannot be applied to intact ligand-gated ion channels, even assuming that it was possible to obtain a sufficient amount of purified material.

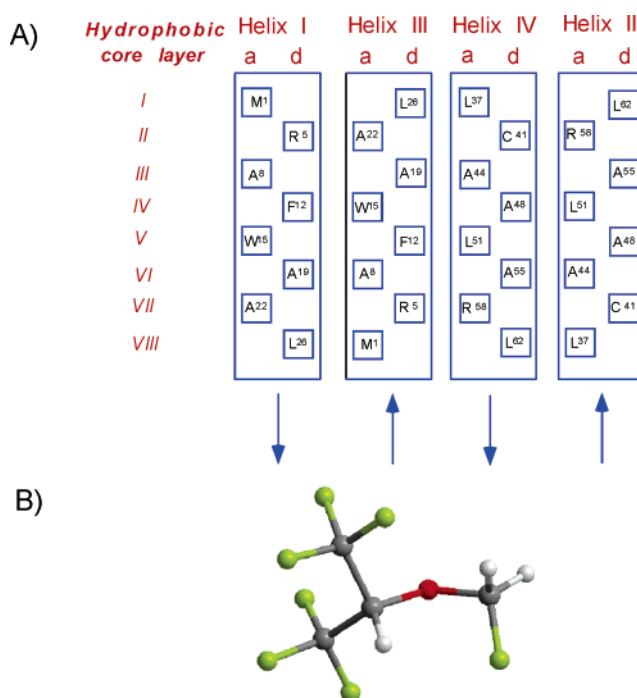


FIGURE 1: (A) An opened-out and flattened representation of the ($\text{A}\alpha_2$ -L1M/L38M)₂ bundle illustrating the residues present at the hydrophobic heptad a and d positions. There are a total of eight hydrophobic core layers, each composed of two a and two d position residues. Equivalent binding sites for anesthetic molecules reside in hydrophobic core layers III and VI where larger leucines were replaced with smaller alanines (43). (B) Ball and stick model of sevoflurane [fluoromethyl 2,2,2-trifluoro-1-(trifluoromethyl)ethyl ether]. Fluorine atoms are in green, carbon atoms are in gray, the oxygen atom is in red, and hydrogen atoms are in white.

[†] Work supported by NIH Grants GM55876 and GM65218.

^{*} Corresponding author. Telephone: 215-349-5472. Fax: 215-349-5078. E-mail: JohanssJ@uphs.upenn.edu.

[‡] Department of Anesthesiology and Critical Care Medicine, University of Pennsylvania.

[§] Department of Biochemistry and Biophysics, University of Pennsylvania.

^{||} Department of Internal Medicine, University of Pennsylvania.

[⊥] Johnson Research Foundation, University of Pennsylvania.

¹ Abbreviations: $\text{A}\alpha_2$, helix-loop-helix peptide; CD, circular dichroism; HSQC, heteronuclear single-quantum coherence; K_d , dissociation constant; kDa, kilodalton; K_{SV} , Stern-Volmer quenching constant; LB, Luria broth; NMR, nuclear magnetic resonance; $[\Theta]_{222}$, molar ellipticity at 222 nm.

Once a volatile general anesthetic binds to a protein, how does its presence lead to a reversible change in protein function? One possibility is that the anesthetic alters either the dynamics or the thermodynamic stability of the protein, shifting a conformational equilibrium so as to favor an open or a closed channel structure. Evidence that volatile general

anesthetic binding can alter both protein stability and dynamics has been obtained with several different model systems (11–14). Alternatively, binding of the anesthetic may cause a structural change in the target protein, but this has been difficult to detect experimentally since it is likely to be quite subtle, given the relatively weak molecular associations that are characteristic of these drugs (15). The only X-ray crystal structure of a complex between a modern volatile general anesthetic and a protein currently available is that of halothane and human serum albumin (16), which uncovered no structural changes following anesthetic binding. In addition, anesthetic-enhanced sodium transport activity by the antimicrobial peptide gramicidin A is not associated with any structural change as assessed by high-resolution nuclear magnetic resonance spectroscopy (17). Further, the limited information on protein architectural changes induced by bound anesthetic molecules indicates that secondary structure is not altered (18, 19). It is therefore likely that a bound anesthetic instead perturbs the tertiary structure of the protein or perhaps the quaternary structure. Only very high-resolution X-ray crystallography will be able to detect the small topological changes that are likely in the case of weakly interacting ligands, such as the volatile general anesthetics. However, if the protein is small enough, spectroscopic approaches may allow structural changes to be detected, as described in this report.

EXPERIMENTAL PROCEDURES

Materials. Sevoflurane [fluoromethyl 2,2,2-trifluoro-1-(trifluoromethyl)ethyl ether] was obtained from Abbott Laboratories (North Chicago, IL). All other chemicals were of reagent grade.

Expression and Purification of $\text{A}\alpha_2\text{-L1M/L38M}$. The $\text{A}\alpha_2\text{-L1M/L38M}$ peptide was expressed and purified as described (20). Peptide identity was confirmed with laser desorption mass spectrometry (Protein Chemistry Laboratory, University of Pennsylvania, Philadelphia, PA). The expected molecular mass was 6863.1 Da, and the experimental value was 6863.0 Da. The uniformly ^{15}N -labeled four- α -helix bundle ($\text{A}\alpha_2\text{-L1M/L38M}$)₂ was obtained by expression from BL21 codon plus (DE3)-RP competent *Escherichia coli* cells. The growth medium for isotopic labeling was M9 minimal medium (21) with modifications: 1 L of medium contained 3.0 g of KH_2PO_4 , 7.0 g of Na_2HPO_4 , 0.5 g of NaCl, 1.0 g of ($^{15}\text{NH}_4$)₂SO₄ (98% ^{15}N from Cambridge Isotope Laboratories, Andover, MA), 1 mM MgSO_4 , 0.1 mM CaCl_2 , 150 μM thiamin, 10 g of D-glucose, and 10 mL of LB medium. Expression and purification of the ^{15}N -labeled four- α -helix bundle ($\text{A}\alpha_2\text{-L1M/L38M}$)₂ was carried out as described (20). The uniformly ^{15}N -labeled $\text{A}\alpha_2\text{-L1M/L38M}$ had a predicted molecular mass of 6944.1 Da and an experimental value of 6947.8 Da.

The overall four- α -helix bundle scaffold was designed to be water-soluble and to have a hydrophobic core as previously described (13, 20, 22, 23). The four- α -helix bundle ($\text{A}\alpha_2\text{-L1M/L38M}$)₂ was assembled from two 62-residue di- α -helical peptides (Figure 1A), each composed of two 27-residue α -helical segments and an eight-residue flexible glycine linker.

Circular Dichroism Spectroscopy. Near-UV spectra were recorded on a Model 62 DS spectropolarimeter (Aviv,

Lakewood, NJ), using a 10 mm path length quartz cell. The cell holder was temperature controlled at 25.0 ± 0.1 °C. The buffer was 130 mM NaCl with 20 mM sodium phosphate at pH 7.0. The bandwidth was 1.00 nm, with a scan step of 0.25 nm and an average scan time of 3.0 s. Far-UV spectra were recorded on the same instrument using a 2 mm path length quartz cell. The cell holder was temperature controlled at 25.0 ± 0.1 °C. The buffer was 10 mM potassium phosphate at pH 7.0. The bandwidth was 1.00 nm, with a scan step of 0.5 nm and an average scan time of 3.0 s.

Steady-State Fluorescence Measurements. Binding of sevoflurane to the four- α -helix bundle ($\text{A}\alpha_2\text{-L1M/L38M}$)₂ was determined using steady-state intrinsic tryptophan fluorescence measurements (18) on a RF-5301PC spectrofluorometer (Shimadzu, Columbia, MD). Tryptophan was excited at 280 nm (bandwidth 1.5 nm), and emission spectra (bandwidth 3 nm) were recorded with the control peak at 324 nm. The quartz cell had a path length of 10 mm and a Teflon stopper. The temperature of the cell holder was controlled at 25.0 ± 0.1 °C. The buffer was 130 mM NaCl and 20 mM sodium phosphate, pH 7.0. Protein concentration was determined with a UV/vis spectrometer Lambda 25 (Perkin-Elmer, Norwalk, CT), taking ϵ_{280} for tryptophan = $5700 \text{ M}^{-1} \text{ cm}^{-1}$ (24). Sevoflurane-equilibrated bundle protein, in gastight Hamilton (Reno, NV) syringes, was diluted with predetermined volumes of plain protein (not exposed to anesthetic but otherwise treated in the same manner) to achieve the final anesthetic concentrations indicated in Figures 2 and 3.

As described previously (18), the quenched fluorescence (Q) is a function of the maximum possible quenching (Q_{max}) at an infinite sevoflurane concentration ([sevoflurane]) and the affinity of the anesthetic for its binding site (K_d) in the vicinity of the tryptophan residues. From mass law considerations, it then follows that

$$Q = (Q_{\text{max}}[\text{sevoflurane}]) / (K_d + [\text{sevoflurane}]) \quad (1)$$

The ability of sevoflurane to directly quench indole fluorescence was examined using *N*-acetyltryptophanamide (Sigma Aldrich Chemical Co., St. Louis, MO) as the model fluorophore, and methanol (Fisher Scientific, Fair Lawn, NJ; spectrophotometric grade) as the solvent, to allow higher concentrations of sevoflurane to be studied. *N*-acetyltryptophanamide was excited at 280 nm (bandwidth 1.5 nm), and emission spectra (bandwidth 3 nm) were recorded with the control peak at 341 nm. The quartz cell had a path length of 10 mm and a Teflon stopper. The temperature of the cell holder was controlled at 25.0 ± 0.1 °C. The *N*-acetyltryptophanamide concentration was determined with a UV/vis spectrometer Lambda 25 (Perkin-Elmer, Norwalk, CT), taking $\epsilon_{280} = 5700 \text{ M}^{-1} \text{ cm}^{-1}$ (24).

Nuclear Magnetic Resonance Measurements. One-dimensional nuclear magnetic resonance spectra were recorded on a Varian Inova 500 MHz instrument with a 90° pulse-acquisition sequence (25) (spectral width of 10 kHz, water presaturated for 1.5 s, 128 scans). The $\text{A}\alpha_2\text{-L1M/L38M}$ concentration was 590 μM in 20 mM phosphate buffer (containing 10% D₂O), pH 7.0. Sevoflurane (50 μL , final concentration 540 μM) was added from a stock solution of 8.0 mM to the NMR tube containing ($\text{A}\alpha_2\text{-L1M/L38M}$)₂ to yield approximately a 1:1 concentration, resulting in a final

$\text{A}\alpha_2\text{-L1M/L38M}$ concentration of $550\ \mu\text{M}$. The spectra were processed using Felix 2.3 from MSI (San Diego, CA) on a Silicon Graphics (Mountain View, CA) workstation. The spectra were referenced with respect to the water peak (4.81 ppm at $20\ ^\circ\text{C}$).

Heteronuclear ^{15}N - ^1H HSQC NMR spectra were recorded at 11.7 T at $25\ ^\circ\text{C}$ on a Varian Inova 500 MHz instrument equipped with a cryoprobe using standard methods (26). The spectra were processed using NMRPipe (27) on a personal computer running the Linux operating system. The spectra were referenced with respect to the water peak (4.78 ppm at $25\ ^\circ\text{C}$).

Gas Chromatography. Buffer concentrations of sevoflurane were determined by gas chromatography on an HP 6890 series instrument (Hewlett-Packard, Wilmington, DE) as described (28).

Gel Filtration. The solution molecular mass of the four- α -helix bundle ($\text{A}\alpha_2\text{-L1M/L38M}$)₂ was determined on a Beckman System Gold HPLC system with a diode array detector (Beckman Coulter Inc., Fullerton, CA) using a TosoHaas (Montgomeryville, PA) G2000SW TSK-GEL column ($300 \times 7.5\ \text{mm}$, $10\ \mu\text{m}$ particle size) and a flow rate of $0.6\ \text{mL/min}$. The elution buffer was $130\ \text{mM}$ NaCl and $20\ \text{mM}$ sodium phosphate, pH 7.0, with or without $2\ \text{mM}$ sevoflurane. Molecular mass standards (all from Sigma Aldrich Chemical Co., St. Louis, MO) consisted of aprotinin ($6.5\ \text{kDa}$), horse heart cytochrome *c* ($12.4\ \text{kDa}$), chymotrypsinogen A ($25.0\ \text{kDa}$), ovalbumin ($43.0\ \text{kDa}$), and bovine serum albumin ($67.0\ \text{kDa}$).

Curve Fitting and Statistics. Best-fit curves were generated with the KaleidaGraph (version 3.6; Synergy Software, Maywood, NJ, 2003) program. Data are expressed as means \pm SD.

RESULTS

The binding of sevoflurane (Figure 1B) to the hydrophobic core of the four- α -helix bundle ($\text{A}\alpha_2\text{-L1M/L38M}$)₂ was followed by tryptophan fluorescence quenching as shown in Figure 2. Sevoflurane causes a concentration-dependent quenching of the intrinsic W15 fluorescence, which is accompanied by a progressive $5\ \text{nm}$ red shift in the emission maximum (from 324 to $329\ \text{nm}$). Since sevoflurane is only a very weak direct quencher of tryptophan fluorescence (see below), the decrease in the quantum yield and the accompanying red shift in the emission maximum are attributed to a conformational change in the hydrophobic core following anesthetic binding. The $58 \pm 1\%$ decrease in the W15 fluorescence quantum yield along with the red shift suggests that the indole ring is reoriented into closer proximity to a quenching carbonyl group of a backbone peptide bond (29). Figure 3a shows a plot of the bundle tryptophan fluorescence as a function of the sevoflurane concentration, yielding a $K_d = 280 \pm 10\ \mu\text{M}$, in agreement with the clinical EC_{50} in man of $260\ \mu\text{M}$ (30).

The importance of bundle tertiary structural interactions for anesthetic binding is shown in Figure 3b, which demonstrates the lack of quenching of W15 fluorescence in the di- α -helical $\text{A}\alpha_2\text{-L1M/L38M}$ by sevoflurane following bundle dissociation with 2,2,2-trifluoroethanol. Trifluoroet-

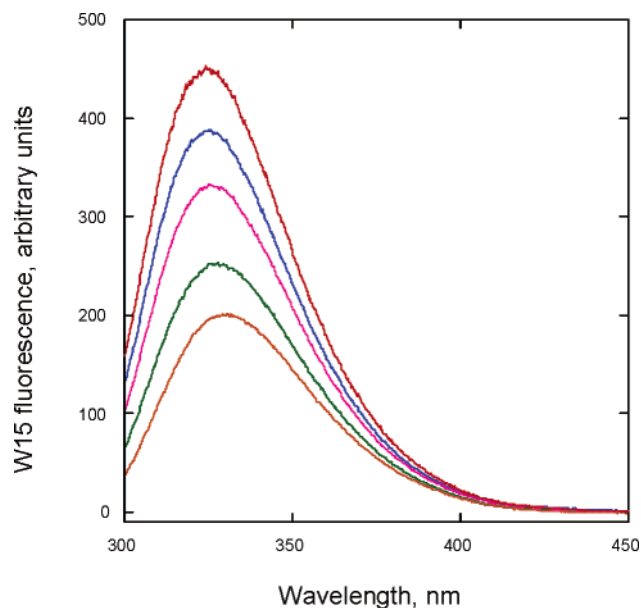


FIGURE 2: Quenching of the ($\text{A}\alpha_2\text{-L1M/L38M}$)₂ bundle ($1.9\ \mu\text{M}$) W15 fluorescence by sevoflurane. Excitation was at $280\ \text{nm}$, with the emission maximum at $324\ \text{nm}$ for the control condition. The concentrations of sevoflurane were (red) 0 , (blue) $80\ \mu\text{M}$, (purple) $240\ \mu\text{M}$, (green) $800\ \mu\text{M}$, and (brown) $8\ \text{mM}$.

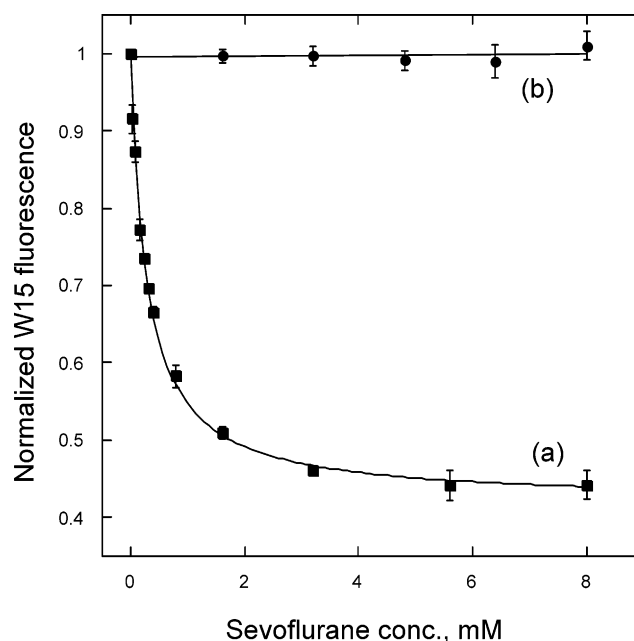


FIGURE 3: (a) Fluorescence quenching profile for the four- α -helix bundle ($\text{A}\alpha_2\text{-L1M/L38M}$)₂ by added sevoflurane. The bundle protein concentration was $1.9\ \mu\text{M}$. Data points are the means of three experiments on separate samples with error bars representing the SD. The line through the data points has the form of eq 1. (b) Effect of sevoflurane on $\text{A}\alpha_2\text{-L1M/L38M}$ ($3.8\ \mu\text{M}$) W15 fluorescence in the presence of 50% ($6.9\ \text{M}$) 2,2,2-trifluoroethanol. Data points are the means of four experiments on separate samples with error bars representing the SD.

hanol negates the hydrophobic interactions that underlie four- α -helix bundle formation, while maintaining secondary structure (31). Because sevoflurane is only a very weak direct quencher of tryptophan fluorescence, no change in the emission intensity is observed under these conditions. This highlights the importance of the intact four- α -helix bundle structure for anesthetic binding. This finding is in line with previous work describing the binding of halothane and

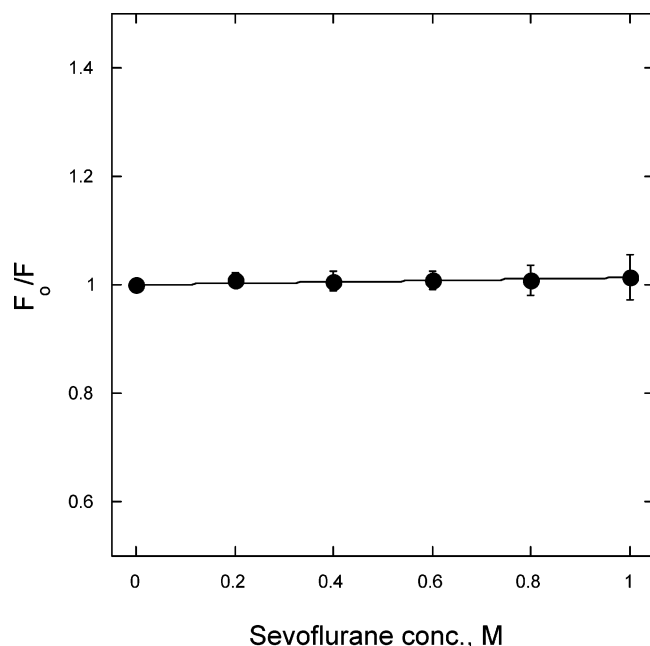


FIGURE 4: Stern–Volmer plot showing the ability of sevoflurane to quench *N*-acetyltryptophanamide fluorescence in methanol. Data points are the means of four experiments with the error bars representing the standard deviations. The line through the data points has the form of $F_0/F = 1 + K_{SV}[\text{sevoflurane}]$, where K_{SV} , the Stern–Volmer quenching constant, has a value of $0.013 \pm 0.002 \text{ M}^{-1}$. F_0 is the fluorescence quantum yield of *N*-acetyltryptophanamide in the absence of sevoflurane, and F is the fluorescence quantum yield of *N*-acetyltryptophanamide in the presence of various concentrations of sevoflurane ($[\text{sevoflurane}]$).

chloroform to the chemically synthesized four- α -helix bundles ($\text{A}\alpha_2\text{-L38M}$)₂ and ($\text{A}\alpha_2\text{-L38M/W15Y}$)₂ (22).

To further test whether sevoflurane might directly quench the fluorescence of W15 in the four- α -helix bundle ($\text{A}\alpha_2\text{-L1M/L38M}$)₂, experiments were performed using the model fluorophore *N*-acetyltryptophanamide and methanol as the solvent in order to allow higher concentrations of sevoflurane to be examined. Figure 4 shows a Stern–Volmer plot of the *N*-acetyltryptophanamide fluorescence intensity as a function of sevoflurane concentration up to 1.0 M. The Stern–Volmer quenching constant, K_{SV} , has a value of $0.013 \pm 0.002 \text{ M}^{-1}$, indicating only minor direct quenching and that a sevoflurane concentration of 76.9 M would be required to decrease the *N*-acetyltryptophanamide fluorescence quantum yield by 50%. To put this into perspective, pure liquid sevoflurane has a concentration of 7.6 M. For comparison, halothane quenches *N*-acetyltryptophanamide fluorescence with $K_{SV} = 47 \pm 2 \text{ M}^{-1}$ (22).

Figure 5 shows the near-UV circular dichroism (CD) spectra of ($\text{A}\alpha_2\text{-L1M/L38M}$)₂ recorded before and after adding increasing concentrations of sevoflurane. The observed CD signal arises from the two phenylalanines (F12 and F52) and one tryptophan (W15) present per monomer. In the wavelength range 255–270 nm, both phenylalanine and tryptophan absorb; hence the near-UV CD in this region reflects the tertiary structure around these three residues (32). Above 270 nm, the near-UV CD reports on the tertiary structure around W15. The addition of sevoflurane leads to clear differences in the near-UV CD signal indicating specific binding to the protein. Below 270 nm, the CD signal changes its sign from positive to negative but retains the same fine

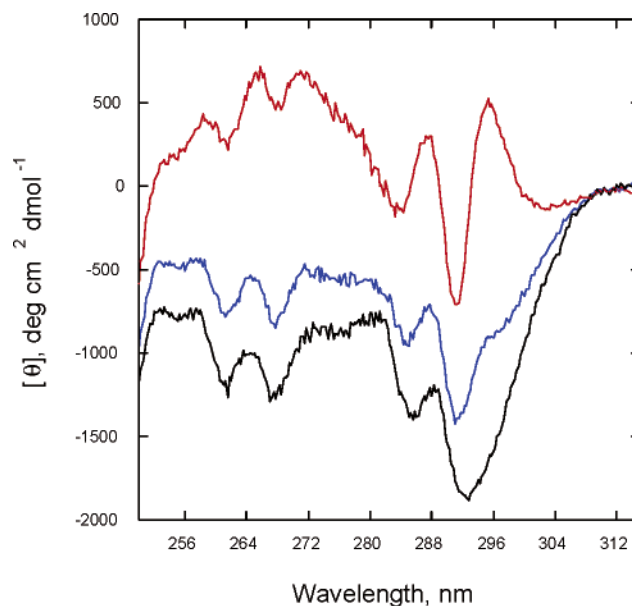


FIGURE 5: Near-UV circular dichroism spectra of ($\text{A}\alpha_2\text{-L1M/L38M}$)₂ at $140 \mu\text{M}$ in 130 mM NaCl and 20 mM sodium phosphate buffer, pH 7.0, and at a temperature of $25.0 \pm 0.1 \text{ }^\circ\text{C}$. The red trace is the control spectrum for ($\text{A}\alpha_2\text{-L1M/L38M}$)₂. Blue and black traces are the spectra obtained after adding $300 \mu\text{M}$ and 2.3 mM sevoflurane, respectively.

structure characteristic of phenylalanine. In the tryptophan region (above 270 nm) there is also a clear effect of sevoflurane binding on ($\text{A}\alpha_2\text{-L1M/L38M}$)₂. In the absence of anesthetic the protein has positive CD signals with maximum intensities at 287 and 295 nm and a negative CD peak centered on 291 nm. In the presence of anesthetic the CD signal becomes negative throughout the tryptophan wavelength range, indicating that this side chain adopts a different conformation compared to that in the absence of anesthetic, in agreement with the fluorescence results.

Far-UV CD spectroscopy was used to determine the effect of sevoflurane on the secondary structure of the four- α -helix bundle ($\text{A}\alpha_2\text{-L1M/L38M}$)₂. Figure 6 shows far-UV CD spectra obtained for ($\text{A}\alpha_2\text{-L1M/L38M}$)₂ in the absence and presence of either 2 mM (a) or 8 mM (b) sevoflurane. The overall shapes of the spectra are typical for a polypeptide with a high α -helical content (33) with positive peaks at 192 nm and two negative peaks at 208 and 222 nm. In Figure 6a, the value of the molar ellipticity at 222 nm is $-22.4 \pm 0.1 (10^{-3} \text{ deg}\cdot\text{cm}^2\cdot\text{dmol}^{-1}, n = 4)$, which is similar to that reported previously for this four- α -helix bundle (20). This translates into a α -helical content of 70.0% using a value of $-32000 \text{ deg}\cdot\text{cm}^2\cdot\text{dmol}^{-1}$ for 100% α -helix (34). The addition of 2 mM sevoflurane produces a small decrease in $[\Theta]_{222} = -22.0 \pm 0.1 (10^{-3} \text{ deg}\cdot\text{cm}^2\cdot\text{dmol}^{-1}, n = 4)$. In contrast, the molar ellipticity at 192 nm increases from a value of $52.4 \pm 0.8 (10^{-3} \text{ deg}\cdot\text{cm}^2\cdot\text{dmol}^{-1}, n = 4)$ in the absence of sevoflurane (Figure 6a) to $53.8 \pm 0.4 (10^{-3} \text{ deg}\cdot\text{cm}^2\cdot\text{dmol}^{-1}, n = 4)$ in the presence of 2 mM sevoflurane. Sevoflurane also red shifts the position of the latter peak on the order of 1 nm. The respective changes in the values of $[\Theta]_{222}$ and $[\Theta]_{192}$ are more pronounced in the presence of 8 mM sevoflurane (Figure 6b). The molar ellipticity at 222 nm is $-22.6 \pm 0.2 (10^{-3} \text{ deg}\cdot\text{cm}^2\cdot\text{dmol}^{-1}, n = 4)$ in the absence of sevoflurane and $-21.9 \pm 0.1 (10^{-3} \text{ deg}\cdot\text{cm}^2\cdot\text{dmol}^{-1}, n = 4)$ in the presence of 8 mM sevoflurane. The molar ellipticity

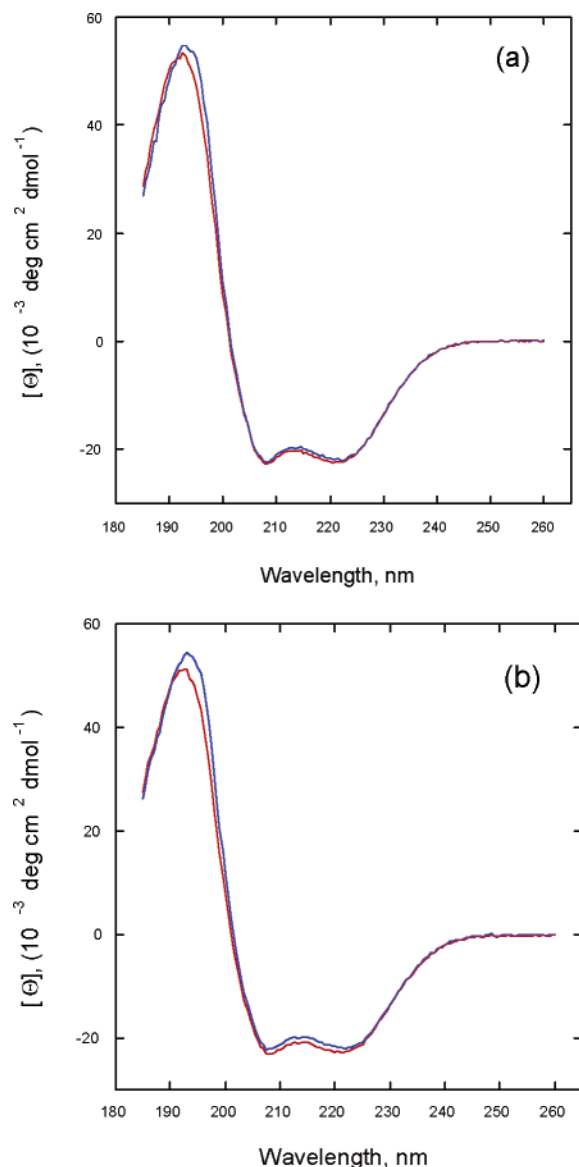


FIGURE 6: Far-UV circular dichroism spectra of $(A\alpha_2-L1M/L38M)_2$ at $5.4 \mu\text{M}$ in 10 mM potassium phosphate buffer, pH 7.0, and at a temperature of $25.0 \pm 0.1^\circ\text{C}$. In each panel, the red trace is the control spectrum for $(A\alpha_2-L1M/L38M)_2$, and the blue traces are in the presence of (a) 2 mM and (b) 8 mM sevoflurane.

at 192 nm is 50.9 ± 0.2 ($10^{-3} \text{ deg} \cdot \text{cm}^2 \cdot \text{dmol}^{-1}$, $n = 4$) in the absence of sevoflurane and 52.8 ± 0.2 ($10^{-3} \text{ deg} \cdot \text{cm}^2 \cdot \text{dmol}^{-1}$, $n = 4$) in the presence of 8 mM sevoflurane.

Figure 7 shows the one-dimensional ^1H NMR spectra of $(A\alpha_2-L1M/L38M)_2$ before (top spectrum) and after adding sevoflurane (bottom spectrum). The spectra are shown in the chemical shift range of 10.5–6 ppm which reports on aromatic and amide protons. In the absence of sevoflurane, the peaks are quite broad and significantly overlapped. This broadness of the resonances may arise from the fact that the protein sequence contains a large degeneracy of amino acid residues (14 glutamates, 12 lysines, 11 leucines, 9 alanines, and 8 glycines, out of a total of 62 amino acids per monomer) and that the four- α -helix bundle exhibits some molten globule character (35). With the addition of sevoflurane the peaks become sharper, indicating that the protein attains a more structured conformation compared to that in the absence of the anesthetic. This is compatible with an anesthetic-induced decrease in protein dynamics.

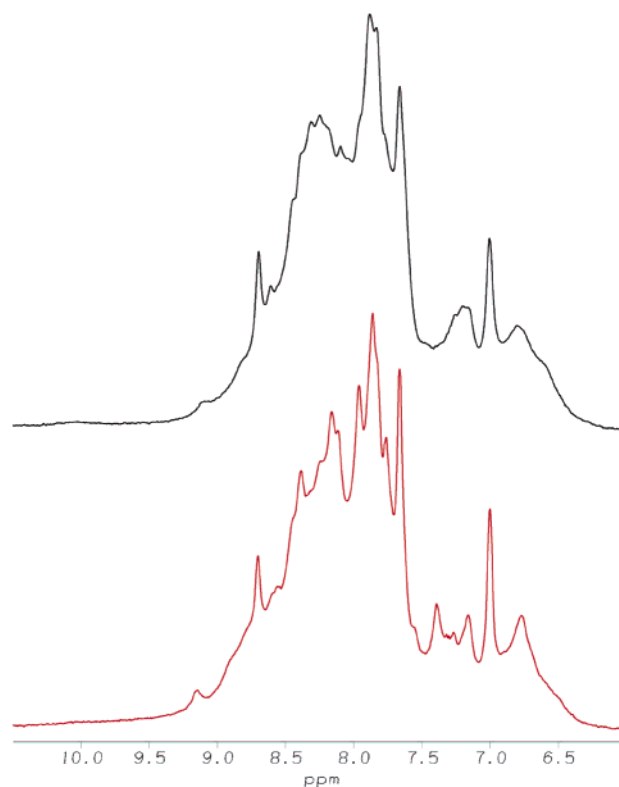


FIGURE 7: One-dimensional ^1H NMR spectra of $A\alpha_2-L1M/L38M$ ($590 \mu\text{M}$) in 20 mM phosphate buffer (90% $\text{H}_2\text{O}/10\% \text{D}_2\text{O}$), pH 7.0, at a temperature of 20°C . The black and red lines represent the spectra before and after adding approximately a 1:1 sevoflurane concentration. Sevoflurane ($540 \mu\text{M}$) was added directly to $A\alpha_2-L1M/L38M$, resulting in a final protein concentration of $550 \mu\text{M}$.

Figure 8 shows the ^{15}N – ^1H heteronuclear single-quantum coherence (HSQC) spectrum of $(A\alpha_2-L1M/L38M)_2$ at 25°C in the absence (blue) and presence (red) of 1 mM sevoflurane. There are differential changes in the intensity of a number of the peaks, with at least 15 of the cross-peaks present in the free protein undergoing chemical shift changes. These observations indicate that a complex is being formed, in line with the fluorescence and circular dichroism data, and that the binding of the anesthetic induces structural changes in the four- α -helix bundle.

Gel filtration was performed in order to determine whether the anesthetic was altering the aggregation state of $(A\alpha_2-L1M/L38M)_2$ and thereby causing the structural changes apparent in Figures 2, 5, 6, 7, and 8. Figure 9 shows chromatograms depicting the elution times of $(A\alpha_2-L1M/L38M)_2$ using a buffer of 130 mM NaCl and 20 mM sodium phosphate, pH 7.0, in the absence (a) and presence of 2 mM sevoflurane (b). On the basis of the molecular mass standards, the $(A\alpha_2-L1M/L38M)_2$ (Figure 9a) has an apparent solution molecular mass of 17.5 kDa. This is not significantly altered in the presence of 2 mM sevoflurane (Figure 9b), indicating that the anesthetic is not altering the aggregation state of the four- α -helix bundle $(A\alpha_2-L1M/L38M)_2$.

DISCUSSION

Conformational changes in a model four- α -helix bundle protein have been demonstrated using three different spectroscopic techniques following the binding of a modern volatile general anesthetic, sevoflurane. Structural changes in proteins following anesthetic binding have been technically

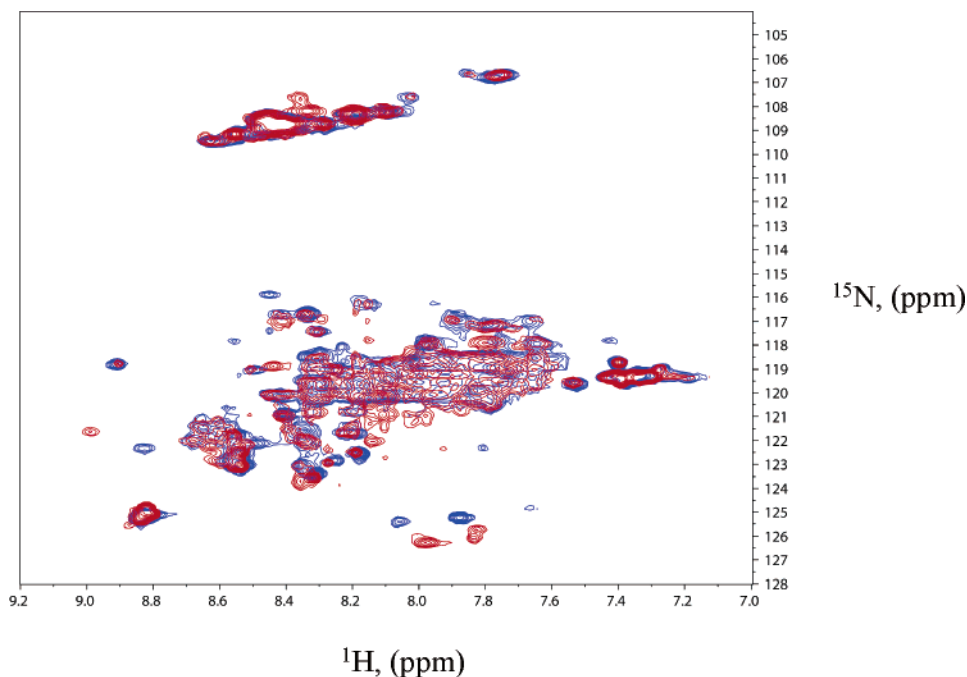


FIGURE 8: Heteronuclear ^{15}N - ^1H HSQC NMR spectrum of $\text{A}\alpha_2\text{-L1M/L38M}$ ($310\ \mu\text{M}$) in 20 mM phosphate buffer (90% H_2O /10% D_2O), pH 4.7, at a temperature of $25\ ^\circ\text{C}$ (blue). The red ^{15}N - ^1H HSQC spectrum was recorded following the addition of 1 mM sevoflurane, which resulted in a final $\text{A}\alpha_2\text{-L1M/L38M}$ concentration of $270\ \mu\text{M}$.

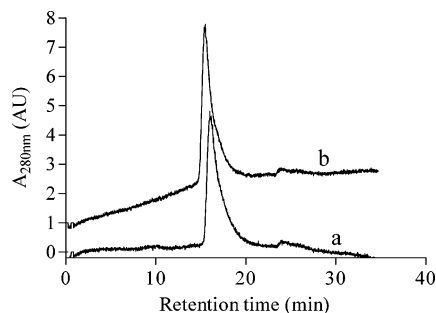


FIGURE 9: Chromatograms depicting the elution times of $(\text{A}\alpha_2\text{-L1M/L38M})_2$ using a buffer of 130 mM NaCl and 20 mM sodium phosphate, pH 7.0, in the absence (a) and presence (b) of 2 mM sevoflurane, monitoring the absorbance at 280 nm. Sevoflurane has no significant effect on the solution molecular mass of the four- α -helix bundle $(\text{A}\alpha_2\text{-L1M/L38M})_2$. Chromatogram b is offset by 1 absorbance unit (vertical direction) for clarity.

difficult to detect (36) but presumably underlie many of the resulting reversible alterations in central nervous system protein function. Comparable structural changes in the predicted in vivo central nervous system protein targets, such as the γ -aminobutyric acid type A receptor and the *N*-methyl-D-aspartate receptor, may underlie some, or all, of the behavioral effects of these widely used clinical agents.

Sevoflurane bound to the hydrophobic core of the four- α -helix bundle $(\text{A}\alpha_2\text{-L1M/L38M})_2$ with a K_d of $280 \pm 10\ \mu\text{M}$, as assessed by changes in the quantum yield of W15. Using isothermal titration calorimetry, sevoflurane bound to the chemically synthesized four- α -helix bundle $(\text{A}\alpha_2\text{-L38M})_2$ with a K_d of $140 \pm 10\ \mu\text{M}$ (37), in reasonable agreement with the current result. For comparison, using ^{19}F NMR spectroscopy, sevoflurane has been shown to bind to bovine serum albumin with a K_d value of $4.5 \pm 0.6\ \text{mM}$ (38). Similarly, using isothermal titration calorimetry, sevoflurane binds to bovine serum albumin with a K_d value of $3.7 \pm 0.4\ \text{mM}$ (39). The current results extend the utility of intrinsic

tryptophan fluorescence studies to allow the binding of a nonquenching, or weakly quenching, volatile general anesthetic to be monitored.

The near-UV circular dichroism spectroscopy results indicate that sevoflurane binding leads to a reorientation of the aromatic residues F12 and W15 in the hydrophobic core of the four- α -helix bundle $(\text{A}\alpha_2\text{-L1M/L38M})_2$. The interfacial heptad e position F52 also apparently alters its orientation upon anesthetic binding. Such changes in side-chain configuration upon anesthetic binding are predicted to have both functional and dynamic consequences and will also have effects on the overall thermodynamic stability of the protein.

The far-UV circular dichroism spectroscopy results indicate that sevoflurane binding also alters the secondary structure of the four- α -helix bundle $(\text{A}\alpha_2\text{-L1M/L38M})_2$. The increase in the molar ellipticity at 192 nm in the presence of sevoflurane is compatible with a slight increase in α -helical content. The decrease in molar ellipticity at 222 nm is not in line with an increase in α -helical content, but aromatic residues also contribute to the spectral intensity in this wavelength region (33), and Figure 5 shows that the orientations of F12, W15, and F52 are altered by anesthetic binding. The 1 nm red shift in the position of the positive 192 nm peak in the far-UV circular dichroism spectrum following sevoflurane binding may reflect the presence of a mixture of 3_{10} - and α -helical regions coexisting in the four- α -helix bundle, since right-handed 3_{10} -helices have a positive peak at 195 nm (40).

The one-dimensional ^1H nuclear magnetic resonance spectroscopy results indicate that sevoflurane binding to the hydrophobic core is associated with a structural tightening of the four- α -helix bundle $(\text{A}\alpha_2\text{-L1M/L38M})_2$. Using hydrogen exchange (13), the volatile general anesthetic halothane was also shown to stabilize the folded conformation of the chemically synthesized four- α -helix bundle $(\text{A}\alpha_2\text{-L38M})_2$. Thus, binding of volatile general anesthetic mol-

ecules to the four- α -helix bundle scaffolds is associated with a stabilization of the folded conformation of the protein. As noted earlier (13), such stabilization of certain protein conformations may represent a common mechanism whereby volatile general anesthetics reversibly perturb normal protein function. In the case of the Cys-loop ligand-gated ion channels such as the γ -aminobutyric acid type A receptor, binding of volatile general anesthetic molecules would therefore be predicted to favor the open conformation of the channel over the closed conformation. In contrast, a large-scale 2.2 ns all-atom molecular dynamics simulation study indicates that halothane increases the root mean square fluctuations of the C α carbons along the backbone of the antimicrobial peptide gramicidin A, suggesting an overall enhancement of channel motions (14).

The two-dimensional ^{15}N – ^1H HSQC nuclear magnetic resonance spectra of the four- α -helix bundle ($\text{A}\alpha_2\text{-L1M/L38M}$)₂ indicate that several NH resonance cross-peaks are shifted or sharpened when sevoflurane binds to the hydrophobic core. Cross-peak shifts in the glycine loop at the ^{15}N 108–109 ppm chemical shift region in Figure 8 indicate that anesthetic binding can cause structural changes at a location distant (on the order of 10 Å) from the actual binding sites in hydrophobic core layers III and VI (Figure 1). Such widespread, but subtle, structural changes upon anesthetic binding are predicted to translate into alterations in normal protein activity, given the close link between protein structure and function (41, 42).

An understanding of volatile general anesthetic mechanisms of action will ultimately require precise structural descriptions of the complexes formed with various protein targets. This continues to remain a technical challenge in the case of a natural ligand-gated ion channel such as the γ -aminobutyric acid type A receptor, because a sufficient amount of pure material is not available. However, ongoing X-ray crystallographic and multidimensional heteronuclear nuclear magnetic resonance studies on the current four- α -helix bundle system should allow a more detailed understanding of these structural changes, providing insight into how volatile general anesthetics reversibly alter protein function in the central nervous system.

ACKNOWLEDGMENT

Mass spectrometry was performed at the Protein Chemistry Laboratory, University of Pennsylvania, Philadelphia, PA.

REFERENCES

- Sebel, P. S., Bowdle, T. A., Ghoneim, M. M., Rampil, I. J., Padilla, R. E., Gan, T. J., and Domino, K. B. (2004) The incidence of awareness during anesthesia: A multicenter United States study, *Anesth. Analg.* 99, 833–839.
- Campagna, J. A., Miller, K. W., and Forman, S. A. (2003) Mechanisms of actions of inhaled anesthetics, *N. Engl. J. Med.* 348, 2110–2124.
- Rudolph, U., and Antkowiak, B. (2004) Molecular and neuronal substrates for general anaesthetics, *Nat. Rev. Neurosci.* 5, 709–720.
- Johansson, J. S. (2005) An update on mechanisms of general anesthesia, *Anesth. Analg.* 100, S40–S42.
- Miyazawa, A., Fujiyoshi, Y., and Unwin, N. (2003) Structure and gating mechanism of the acetylcholine receptor pore, *Nature* 423, 949–955.
- Unwin, N. (2005) Refined structure of the nicotinic acetylcholine receptor at 4 Å resolution, *J. Mol. Biol.* 346, 967–989.
- Eckenhoff, R. G. (1996) An inhalational anesthetic binding domain in the nicotinic acetylcholine receptor, *Proc. Natl. Acad. Sci. U.S.A.* 93, 2807–2810.
- Chiara, D. C., Dangott, L. J., Eckenhoff, R. G., and Cohen, J. B. (2003) Identification of nicotinic acetylcholine receptor amino acids photolabeled by the volatile anesthetic halothane, *Biochemistry* 42, 13457–13467.
- Nishikawa, K., and Harrison, N. L. (2003) The actions of sevoflurane and desflurane on the γ -aminobutyric acid receptor type A, *Anesthesiology* 99, 678–684.
- Ishizawa, Y., Pidikiti, R., Liebman, P. A., and Eckenhoff, R. G. (2002) G protein-coupled receptors as direct targets of inhaled anesthetics, *Mol. Pharmacol.* 61, 945–952.
- Eckenhoff, R. G., and Tanner, J. W. (1998) Differential halothane binding and effects on serum albumin and myoglobin, *Biophys. J.* 75, 477–483.
- Johansson, J. S., Zou, H., and Tanner, J. W. (1999) Bound volatile general anesthetics alter both local protein dynamics and global protein stability, *Anesthesiology* 90, 235–245.
- Johansson, J. S., Scharf, D., Davies, L. A., Reddy, K. S., and Eckenhoff, R. G. (2000) A designed four- α -helix bundle that binds the volatile general anesthetic halothane with high affinity, *Biophys. J.* 78, 982–993.
- Tang, P., and Xu, Y. (2002) Large-scale molecular dynamics simulations of general anesthetic effects on the ion channel in the fully hydrated membrane: The implication of molecular mechanisms of general anesthesia, *Proc. Natl. Acad. Sci. U.S.A.* 99, 16035–16040.
- Eckenhoff, R. G., and Johansson, J. S. (1997) Molecular interactions between inhaled anesthetics and proteins, *Pharmacol. Rev.* 49, 343–367.
- Bhattacharya, A. A., Curry, S., and Franks, N. P. (2000) Binding of the general anesthetics propofol and halothane to human serum albumin, *J. Biol. Chem.* 275, 38731–38738.
- Tang, P., Mandal, P. K., and Zegarar, M. (2002) Effects of volatile anesthetic on channel structure of gramicidin A, *Biophys. J.* 83, 1413–1420.
- Johansson, J. S., Eckenhoff, R. G., and Dutton, P. L. (1995) Binding of halothane to serum albumin demonstrated using tryptophan fluorescence, *Anesthesiology* 83, 316–324.
- Johansson, J. S. (1997) Binding of the volatile anesthetic chloroform to albumin demonstrated using tryptophan fluorescence quenching, *J. Biol. Chem.* 272, 17961–17965.
- Pidikiti, R., Shamin, M., Mallela, K. M. G., Reddy, K. S., and Johansson, J. S. (2005) Expression and characterization of a four- α -helix bundle protein that binds the volatile general anesthetic halothane, *Biomacromolecules* 6, 1516–1523.
- Miller, J. H. (1972) *Experiments in Molecular Genetics*, Cold Spring Harbor Laboratory Press, Cold Spring Harbor, NY.
- Manderson, G. A., and Johansson, J. S. (2002) Role of aromatic side chains in the binding of volatile general anesthetics to a four- α -helix bundle, *Biochemistry* 41, 4080–4087.
- Manderson, G. A., Michalsky, S. J., and Johansson, J. S. (2003) Effect of four- α -helix bundle cavity size on volatile anesthetic binding energetics, *Biochemistry* 42, 11203–11213.
- Edelhoch, H. (1967) Spectroscopic determination of tryptophan and tyrosine in proteins, *Biochemistry* 6, 1948–1954.
- Cavanagh, J., Fairbrother, W. J., Palmer, A. G., and Skelton, N. J. (1996) *Protein NMR Spectroscopy: Principles and Practice*, Academic Press, San Diego, CA.
- Fesik, S. W., and Zuiderweg, E. R. P. (1988) Heteronuclear three-dimensional NMR spectroscopy. A strategy for the simplification of homonuclear two-dimensional NMR spectra, *J. Magn. Reson.* 78, 588–593.
- Delaglio, F., Grzesiek, S., Vuister, G. W., Zhu, G., Pfeifer, J., and Bax, S. (1995) NMRPipe: A multidimensional spectral processing system based on UNIX pipes, *J. Biomol. NMR* 6, 277–293.
- Johansson, J. S., Rabanal, F., and Dutton, P. L. (1996) Binding of the volatile anesthetic halothane to the hydrophobic core of a tetra- α -helix bundle protein, *J. Pharmacol. Exp. Ther.* 279, 56–61.

29. Pan, C.-P., and Barkley, M. D. (2004) Conformational effects on tryptophan fluorescence in cyclic hexapeptides, *Biophys. J.* **86**, 3828–3835.
30. Krasowski, M. D., and Harrison, N. L. (1999) General anaesthetic actions on ligand-gated ion channels, *Cell. Mol. Life Sci.* **55**, 1278–1303.
31. Buck, M. (1998) Trifluoroethanol and colleagues: Cosolvents come of age. Recent studies with peptides and proteins, *Q. Rev. Biophys.* **31**, 297–355.
32. Kelly, S. M., and Price, N. C. (2000) The use of circular dichroism in the investigation of protein structure and function, *Curr. Protein Pept. Sci.* **1**, 349–384.
33. Woody, R. W. (1995) Circular dichroism, *Methods Enzymol.* **246**, 34–71.
34. Lau, S. Y. M., Taneja, A. K., and Hodges, R. S. (1984) Synthesis of a model protein of defined secondary and quaternary structure, *J. Biol. Chem.* **259**, 13253–13261.
35. Gibney, B. R., Rabanal, F., Skalicky, J. J., Wand, A. J., and Dutton, P. L. (1999) Iterative protein redesign, *J. Am. Chem. Soc.* **121**, 4952–4960.
36. Johansson, J. S., and Eckenhoff, R. G. (2002) *Protein Models in Neural Mechanisms of Anesthesia*, Humana Press, Totowa, NJ.
37. Zhang, T., and Johansson, J. S. (2003) An isothermal titration calorimetry study on the binding of four volatile general anesthetics to the hydrophobic core of a four- α -helix bundle protein, *Biophys. J.* **85**, 3279–3285.
38. Dubois, B. W., Cherian, S. F., and Evers, A. S. (1993) Volatile anesthetics compete for common binding sites on bovine serum albumin: A ^{19}F NMR study, *Proc. Natl. Acad. Sci. U.S.A.* **90**, 6478–6482.
39. Sawas, A. H., Pentiyala, S. N., and Rebecchi, M. J. (2004) Binding of volatile anesthetics to serum albumin: Measurements of enthalpy and solvent contributions, *Biochemistry* **43**, 12675–12685.
40. Toniolo, C., Polese, A., Formaggio, F., Crisma, M., and Kamphuis, J. (1996) Circular dichroism spectrum of a peptide 3_{10} -helix, *J. Am. Chem. Soc.* **118**, 2744–2745.
41. Mesecar, A. D., Stoddard, B. L., and Koshland, D. E. (1997) Orbital steering in the catalytic power of enzymes: Small structural changes with large catalytic consequences, *Science* **277**, 202–206.
42. Peracchi, A. (2001) Enzyme catalysis: Removing chemically “essential” residues by site-directed mutagenesis, *Trends Biochem. Sci.* **26**, 497–503.
43. Johansson, J. S., Gibney, B. R., Rabanal, F., Reddy, K. S., and Dutton, P. L. (1998) A designed cavity in the hydrophobic core of a four- α -helix bundle improves volatile anesthetic binding affinity, *Biochemistry* **37**, 1421–1429.

BI050896Q